Dynamic polarization potentials and dipole polarizabilities of ^{11}Li, ^{6}He and ^{6}Li compared

N. Keeley,[1,*] K. W. Kemper,[2,3] and K. Rusek[1,3]

[1]*National Centre for Nuclear Research, ul. Andrzeja Sołtana 7, 05-400 Otwock, Poland*

[2]*Department of Physics, The Florida State University, Tallahassee, Florida 32306, USA*

[3]*Heavy Ion Laboratory, University of Warsaw, ul. Pasteura 5A, 02-093 Warsaw, Poland*

(Received 29 May 2013; revised manuscript received 3 July 2013; published 22 July 2013)

Elastic scattering data for ^{11}Li, ^{6}Li, and ^{6}He + ^{208}Pb at incident energies of 29.8 MeV, 29 MeV, and 18 MeV, respectively, were analyzed by means of coupled discretized continuum channels (CDCC) calculations. Dynamic polarization potentials (DPPs) of the trivially equivalent local potential (TELP) type were derived from these calculations and compared. The dipole polarizability factor α for ^{11}Li obtained by fitting a Coulomb polarization potential to the long-range part of the real DPP is consistent with the theoretical value of 5.7 fm^3. These results point to the dineutron model providing a very good description of ^{11}Li breakup coupling effects. The much larger Coulomb dipole polarizability of ^{11}Li suggests the persistence of large deviations from Rutherford scattering at sub-barrier energies for medium mass targets, a prediction confirmed by CDCC calculations.

DOI: 10.1103/PhysRevC.88.017602 PACS number(s): 25.60.Bx, 25.60.Je, 24.10.Eq, 25.70.Bc

A recent measurement [1] of the elastic scattering of ^{11}Li by a ^{208}Pb target at incident energies below the nominal Coulomb barrier found angular distributions that deviated markedly from Rutherford scattering, in contrast to the behavior of "normal" heavy-ion scattering. Four-body coupled discretized continuum channels (CDCC) calculations were able to describe the data well and indicated that the main cause of the large deviation from Rutherford scattering was Coulomb dipole coupling, which may in turn be associated with a large Coulomb dipole polarizability of ^{11}Li. In this work we employ a two-body dineutron model of ^{11}Li to perform CDCC calculations for the data of Ref. [1] and compare the results with calculations for ^{6}Li + ^{208}Pb and ^{6}He + ^{208}Pb at similar energies with respect to the Coulomb barrier (29 MeV and 18 MeV, respectively). These nuclei make excellent comparisons with ^{11}Li, since ^{6}He has a large dipole polarizability (see, e.g., Parkar *et al.* [2], and references therein) whereas the dipole couplings in ^{6}Li are negligible (identically zero in a strict $\alpha + d$ model). Dynamic polarization potentials (DPPs) of the trivially equivalent local potential (TELP) type were derived from the CDCC calculations and compared at large radii. The long range parts of the real DPPs for ^{11}Li and ^{6}He were well reproduced by Coulomb polarization potentials, thus enabling the dipole polarizability factors to be compared with each other and theory. This procedure [3] was adopted rather than direct fitting of the elastic scattering data with a parametrized DPP (as was done in Ref. [2] for example) due to the scatter in the ^{11}Li + ^{208}Pb data (see Fig. 1) leading to a wide range of possible potentials of this type. All calculations were carried out using the code FRESCO [4].

We adopted a simplified two-body model of ^{11}Li since it retains the essential physics of the problem while avoiding the complications of the more sophisticated three-body model used in Ref. [1]. Although several low-lying resonances have been identified in ^{11}Li [5] we did not include these since they have no definite spin-parity assignments as yet. To keep the size of the ^{11}Li calculation within reasonable bounds we set the spin of the ^{9}Li core equal to zero. The ^{11}Li diagonal and coupling potentials were calculated using Watanabe-type folding. The ^{2}n + ^{9}Li binding potential was of Woods-Saxon form with parameters: $R = 0.66(2^{1/3} + 9^{1/3})$ fm, $a = 0.2$ fm, the depth being adjusted to give the correct two-neutron separation energy of 0.37 MeV. The deuteron potential of Ref. [6] was used for the ^{2}n + ^{208}Pb optical potential and the ^{7}Li potential of Ref. [7] for the ^{9}Li + ^{208}Pb optical potential (the ^{9}Li elastic scattering at the required energy, 24.4 MeV, is very close to pure Rutherford scattering [1], therefore the ^{11}Li calculation is relatively insensitive to the choice of ^{9}Li + ^{208}Pb optical potential). The ^{2}n + ^{9}Li continuum was divided into bins in momentum (k) space of width $\Delta k = 0.1$ fm^{-1} up to a maximum value of $k_{\max} = 0.7$ fm $^{-1}$. Relative angular momenta $L = 0, 1, 2, 3$ were included with all couplings up to multipolarity $\lambda = 3$. The ^{6}He + ^{208}Pb calculations were similar to those of Ref. [8] using the improved dineutron model of ^{6}He of Ref. [9], with the exception that relative angular momentum values up to $L = 4$ and couplings up to multipolarity $\lambda = 4$ were included, although tests found that the extra bins and couplings had a negligible effect on the DPP in the radial region under discussion here. The ^{6}Li + ^{208}Pb calculations were similar to those described in Ref. [10] with the continuum binning truncated at $k_{\max} = 0.8$ fm^{-1}. The d + ^{208}Pb and α + ^{208}Pb optical potentials were taken from Refs. [6] and [11], respectively.

In Fig. 1 we compare the calculations with the data for ^{11}Li, ^{6}Li, and ^{6}He + ^{208}Pb elastic scattering at 29.8 MeV [1], 29 MeV [12], and 18 MeV [13].

The agreement between calculations and data validates the models used as representing the effects of breakup coupling sufficiently realistically to describe the available data. In particular, the coupling effect for ^{11}Li is qualitatively similar to that of Ref. [1]. We also show in Fig. 1 the results of CDCC calculations without Coulomb couplings (but retaining the diagonal Coulomb potentials) as the dotted curves. It will be noted that while the coupling effect for ^{11}Li and ^{6}He is dominated by Coulomb coupling (cf. the solid and dotted

*keeley@fuw.edu.pl

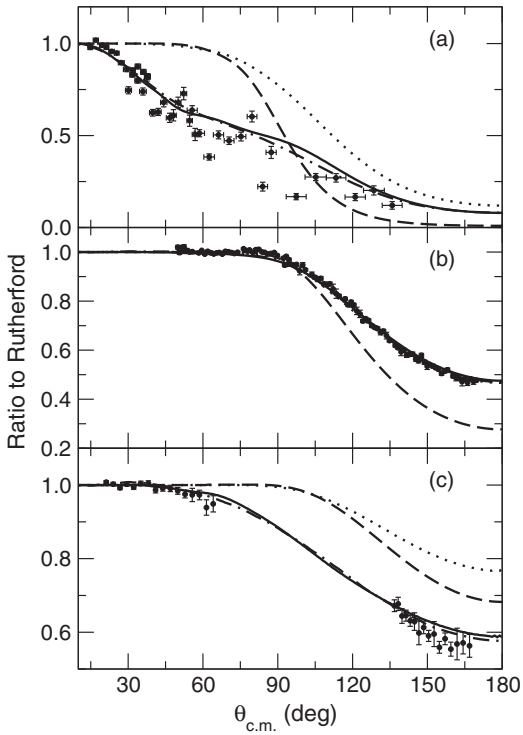

FIG. 1. CDCC calculations compared to the elastic scattering data for: (a) 29.8 MeV ^{11}Li + ^{208}Pb, (b) 29 MeV ^{6}Li + ^{208}Pb, and (c) 18 MeV ^{6}He + ^{208}Pb. The solid and dashed curves represent the results of the full CDCC and no-coupling calculations, respectively. The dotted curves denote the results of CDCC calculations with no Coulomb couplings (but retaining the diagonal Coulomb potentials). The dot-dashed curves denote the results of optical model calculations with the bare potentials + DPPs, see text. Note the linear cross section scale.

curves), for ^{6}Li the Coulomb coupling has a negligible effect, as found previously [14,15] [the dotted curve on Fig. 1(b) is barely visible]. The total (Coulomb plus nuclear) coupling effect is also qualitatively different for ^{6}Li, which may be ascribed to the absence of strong Coulomb dipole coupling in this nucleus.

Coupling effects may be represented by a potential term—the dynamic polarization potential or DPP—added to the "bare" optical potential used as input to the coupled channels calculation. This DPP is intrinsically nonlocal and L-dependent, but local, L-independent equivalents may always be found. In this work we use one such local equivalent DPP, the so-called trivially equivalent local potential of Ref. [16], as implemented in the code FRESCO [4]. In Fig. 2 we present the TELP-type DPPs derived from the CDCC calculations for ^{11}Li, ^{6}He and ^{6}Li at large radii. As a check on the validity of these DPPs, at least in the region where the elastic scattering is sensitive to the potential, we plot in Fig. 1 as the dot-dashed curves the angular distributions predicted by optical model calculations employing the bare potential plus the DPP. The agreement with the CDCC calculations is good (in the case of ^{6}Li so good that the dot-dashed curve is completely hidden) thus validating the DPPs as a representation of the coupling effects. A significant qualitative difference between the DPPs

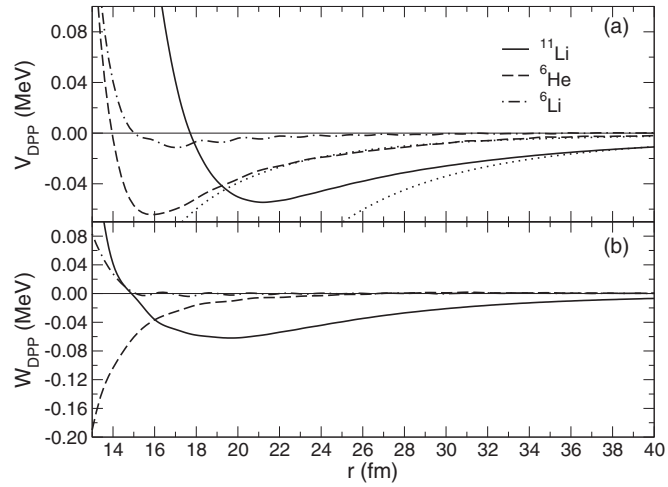

FIG. 2. TELP-type DPPs derived from the CDCC calculations for ^{11}Li, ^{6}He, and ^{6}Li + ^{208}Pb. The dotted curves in (a) denote the Coulomb polarization potential of Eq. (1) with values of $\alpha = 5.7$ fm^3 and 1.3 fm^3 for ^{11}Li and ^{6}He, respectively.

for ^{11}Li and ^{6}He and that for ^{6}Li is immediately apparent: while the ^{11}Li and ^{6}He DPPs both exhibit the long attractive and absorptive tails characteristic of strong dipole Coulomb couplings [8,17–19], the ^{6}Li DPP is essentially zero for radii $r > 20$ fm ($r > 15$ fm for the imaginary part). Given that in the $\alpha + d$ model of ^{6}Li dipole couplings are identically zero this behavior is to be expected and may be adduced as further evidence that the long tails in the ^{11}Li and ^{6}He DPPs do indeed result from the Coulomb dipole coupling to the continuum.

The long-range tails of the ^{11}Li and ^{6}He real DPPs may therefore be represented by the Coulomb polarization potential given by

$$V_{\rm Pol}(r) = -\frac{1}{2}\alpha\frac{Z_{\rm T}^2 e^2}{r^4}, \qquad (1)$$

where α is the Coulomb dipole polarizability parameter, $Z_{\rm T}$ the target atomic number, and e the charge on the electron. The ^{6}He real DPP is consistent with a value of $\alpha \sim 1.3$ fm^3, somewhat smaller than the theoretical values of 1.88 fm^3 [20] or 1.99 fm^3 [21] but close to the value of 1.2 fm^3 obtained in Ref. [2], while the ^{11}Li real DPP is consistent with the theoretical value of $\alpha = 5.7$ fm^3 [22]. The good agreement of the "empirical" dipole polarizability with theory suggests that the dineutron model is a much better approximation for ^{11}Li than it is for ^{6}He, implying a stronger correlation between the two valence neutrons in ^{11}Li (it will be recalled that we have used the improved dineutron model of Ref. [9] for ^{6}He which better matches the wave functions from more sophisticated three-body models; the "pure" dineutron model significantly overpredicts the dipole strength for ^{6}He, as was demonstrated in Ref. [9])

The long-range absorptive tail of the ^{11}Li imaginary DPP also extends to much larger radii than that for ^{6}He, suggesting that the Coulomb breakup of ^{11}Li takes place further from the target. This may be explained as due to the larger size of ^{11}Li. However, since the difference between the rms matter radii of ^{11}Li and ^{6}He is only of the order of 1.4 fm or so, the difference

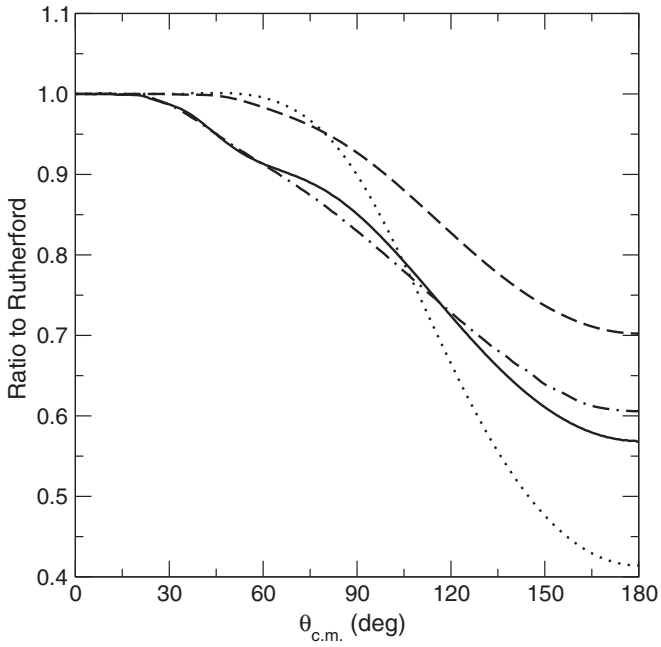

FIG. 3. CDCC calculations for 11.6 MeV ^{11}Li + ^{58}Ni elastic scattering. The solid and dashed curves represent the results of the full CDCC and no-coupling calculations, respectively. The dotted curve denotes the result of a CDCC calculation with no Coulomb couplings (but retaining the diagonal Coulomb potentials). The dot-dashed curve denotes the result of an optical model calculation with the bare potential + DPP. Note the linear cross section scale.

in the imaginary DPPs suggests a greater extent of the neutron halo distribution for ^{11}Li as the probable cause of this very long range absorption. Test calculations for ^{11}Li + ^{208}Pb where the TELP-type DPP was replaced by the forms of Eq. (1) for both real and imaginary parts for $r > 24$ fm (and kept constant at the value for $r = 24$ fm for $r < 24$ fm) found that the CDCC angular distribution was well reproduced for center-of-mass angles $\theta_{\text{c.m.}} \leqslant 75^\circ$. For $\theta_{\text{c.m.}} > 75^\circ$ the repulsive core of the real part of the TELP-type DPP seen in Fig. 2(a) was important.

The very much larger dipole polarizability of ^{11}Li compared to that of ^{6}He suggests that the observed large deviations from Rutherford scattering for sub-barrier ^{11}Li + ^{208}Pb elastic scattering [1] should persist for medium mass targets, unlike the situation for ^{6}He which exhibits normal Fresnel scattering for such targets [23,24]. In Fig. 3 we show the results of CDCC calculations for 11.6 MeV ^{11}Li + ^{58}Ni, a roughly similar energy with respect to the nominal Coulomb barrier as the ^{11}Li + ^{208}Pb data of Ref. [1] shown in Fig. 1(a).

This confirms that even for medium mass targets the complete wiping out of the Coulomb rainbow, the most striking feature of the large breakup coupling effect, does indeed persist for ^{11}Li. In this respect it is similar to ^{11}Be, cf. the ^{11}Be + ^{64}Zn quasielastic scattering data of Ref. [25]. Figure 3 shows that for ^{11}Li the Coulomb breakup coupling remains dominant in the suppression of the Coulomb rainbow for medium mass targets.

In summary, we have shown that a two-body dineutron model of ^{11}Li is able to describe rather well the elastic scattering data for ^{11}Li + ^{208}Pb at an incident energy just below the nominal Coulomb barrier. The long-range attractive real DPP derived from this calculation is consistent with the theoretical dipole polarizability for ^{11}Li, further supporting the suggestion that the dineutron model is more realistic for ^{11}Li than it is for ^{6}He. The much larger dipole polarizability of ^{11}Li compared to that of ^{6}He suggests that the large deviations from Rutherford scattering observed for sub-barrier ^{11}Li + ^{208}Pb elastic scattering should persist for medium mass targets, a prediction confirmed by CDCC calculations.

The authors would like to thank Prof. K. Pachucki of the University of Warsaw for fruitful discussions and communicating the result of his dipole polarizability calculation for ^{11}Li. K.W.K. acknowledges partial support from the Florida State University Robert O. Lawton Fund.

[1] M. Cubero *et al.*, Phys. Rev. Lett. **109**, 262701 (2012).
[2] V. V. Parkar, I. Martel, A. M. Sánchez-Benítez, L. Acosta, K. Rusek, L. Standylo, and N. Keeley, Acta Phys. Pol. B **42**, 761 (2011).
[3] K. Rusek, Eur. Phys. J. A **41**, 399 (2009).
[4] I. J. Thompson, Comput. Phys. Rep. **7**, 167 (1988).
[5] J. H. Kelley, E. Kwan, J. E. Purcell, C. G. Sheu, and H. R. Weller, Nucl. Phys. A **880**, 88 (2012).
[6] C. M. Perey and F. G. Perey, Phys. Rev. **132**, 755 (1963).
[7] J. Cook, Nucl. Phys. A **388**, 153 (1982).
[8] R. S. Mackintosh and N. Keeley, Phys. Rev. C **79**, 014611 (2009).
[9] A. M. Moro, K. Rusek, J. M. Arias, J. Gómez-Camacho, and M. Rodríguez-Gallardo, Phys. Rev. C **75**, 064607 (2007).
[10] C. Beck, N. Keeley, and A. Diaz-Torres, Phys. Rev. C **75**, 054605 (2007).
[11] G. Goldring, M. Samuel, B. A. Watson, M. C. Bertin, and S. L. Tabor, Phys. Lett. B **32**, 465 (1970).
[12] N. Keeley, S. J. Bennett, N. M. Clarke, B. R. Fulton, G. Tungate, P. V. Drumm, M. A. Nagarajan, and J. S. Lilley, Nucl. Phys. A **571**, 326 (1994).
[13] A. M. Sánchez-Benítez *et al.*, Nucl. Phys. A **803**, 30 (2008).
[14] N. Keeley and K. Rusek, Phys. Lett. B **427**, 1 (1998).
[15] H. Kumawat, V. Jha, B. J. Roy, V. V. Parkar, S. Santra, V. Kumar, D. Dutta, P. Shukla, L. M. Pant, A. K. Mohanty, R. K. Choudhury, and S. Kailas, Phys. Rev. C **78**, 044617 (2008).
[16] M. A. Franey and P. J. Ellis, Phys. Rev. C **23**, 787 (1981).

[17] R. S. Mackintosh and N. Keeley, Phys. Rev. C **70**, 024604 (2004).
[18] N. Keeley and R. S. Mackintosh, Phys. Rev. C **71**, 057601 (2005).
[19] O. R. Kakuee, M. A. G. Alvarez, M. V. Andres, S. Cherubini, T. Davinson, A. Di Pietro, W. Galster, J. Gómez-Camacho, A. M. Laird, M. Lamehi-Rachti, I. Martel, A. M. Moro, J. Rahighi, A. M. Sánchez-Benitez, A. C. Shotter, W. B. Smith, J. Vervier, and P. J. Woods, Nucl. Phys. A **765**, 294 (2006).
[20] J. A. Lay, A. M. Moro, J. M. Arias, and J. Gómez-Camacho, Phys. Rev. C **82**, 024605 (2010).
[21] K. Pachucki and A. M. Moro, Phys. Rev. A **75**, 032521 (2007).
[22] K. Pachucki (private communication).
[23] A. Di Pietro *et al*., Phys. Rev. C **69**, 044613 (2004).
[24] Y. Kucuk, I. Boztosun, and N. Keeley, Phys. Rev. C **79**, 067601 (2009).
[25] A. Di Pietro *et al*., Phys. Rev. Lett. **105**, 022701 (2010).